 doi:10.20944/preprints202210.0143.v1

Article

A Composite Exponential Reaching Law based SMC with Rotating Sliding Surface Selection Mechanism for Two Level Three Phase VSI in Vehicle to Load Applications

Faheem Haroon[1], Muhammad Aamir[2], Assad Waqar[1*], Saeed Mian Qaisar[3*], Syed Umaid Ali[1], Abdulaziz Turki Almaktoom[4*]

[1] Department of Electrical Engineering, Bahria School of Engineering & Applied Sciences Islamabad Campus (BSEAS-IC), Islamabad 44000, Pakistan; faheemharoon.buic@bahria.edu.pk (F.H.); sumaid.buic@bahria.edu.pk (S.U.A.)
[2] Pak-Austria Fachhochschule: Institute of Applied Sciences and Technology, Haripur 22620, Pakistan; muhammad.aamir@fecid.paf-iast.edu.pk (M.A.)
[3] Electrical and Computer Engineering Department, Effat University, Jeddah, 22332, Saudi Arabia
[4] Supply Chain Management Department, Effat University, Jeddah, 22332, Saudi Arabia
* Correspondence: asadwaqar.buic@bahria.edu.pk (A.W.); sqaisar@effatuniversity.edu.sa (S.M.Q.) ; abalmaktoom@effatuniversity.edu.sa (A.T.A.)

Abstract: Voltage Source Inverters (VSI) are the integral part of Electrical Vehicles (EV) to enhance the reliability of supply power to critical loads in vehicle to load (V2L) applications. Inherent properties of sliding mode control (SMC) makes it one of the best vailable options to achieve desired voltage quality under variable load conditions. Intrinsic characteristic of robustness associated with SMC is achieved generally at the cost of unwanted chattering along the sliding surface. To manage this compromise better, optimal selection of sliding surface coefficient is applied with proposed composite exponential reaching law (C-ERL). The novelty of proposed C-ERL is associated with the intelligent mix of exponential, power and difference functions blended with rotating sliding surface selection (RSS) technique for three phase two level VSI. Moreover, proposed reaching law along with power rate exponential reaching law(PRERL), enhanced exponential reaching law(EERL) and repeatitive reaching law(RRL) are implemented on two level three phase VSI under variable load condtions. Comparative analysis of which strongly advocates the authenticity and effectiveness of proposed reaching law in achieving well regulated output voltage, with high level of robustness, reduced chattering and low %THD.

Keywords: Sliding Mode Control; Three phase Voltage Source Inverter; Reaching Law; Chattering; Sliding Surface.

1. Introduction

Electrical vehicles (EV) in vehicle to load(V2L) mode of operation is considered one of the best ways to enhance the reliability of supply to critical loads like medical equipment in hospitals, military loads, communication systems, data processing and storage systems etc [1-3]. In V2L mode of operation, EV ensures uninterrupted power supply to critical loads in-case of main grid failure and operates in stand-alone mode for electrification of utilities and expensive loads in remote areas [4-6]. Nowadays, EV uses more or less similar power electronic interface to derive critical loads in V2L i-e three phase two level voltage source inverter (TLVSIs) [7]. In order to handle sensitivity associated with critical loads, three phase TLVSI must have high disturbance rejection capacity, exceptional voltage regulation with low total harmonic distortion (%THD), fast transient and excellent dynamic response under sudden load variations [8].

Preprints (www.preprints.org) | NOT PEER-REVIEWED | Posted: 11 October 2022 doi:10.20944/preprints202210.0143.v1

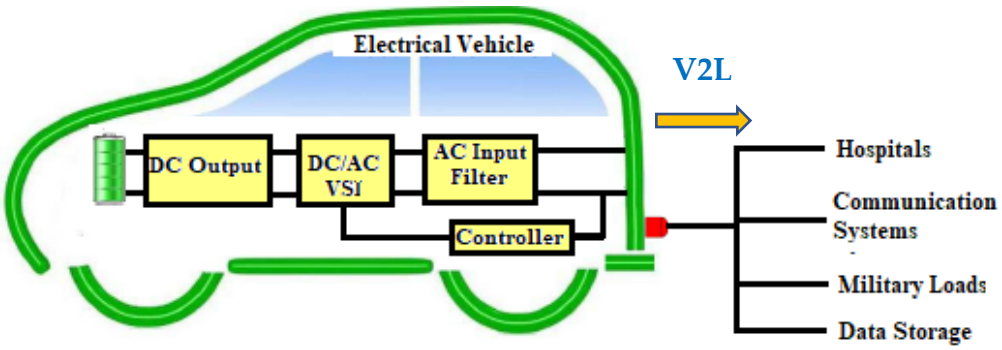

Figure 1. Schematic of V2L operation of system.

In today's world, operations of systems associated with voltage source inverter (VSI) are meeting stability constraints to overcome economic and environmental concerns. Intrinsic properties of sliding mode control (SMC) like high robustness, simple design and reduced order makes it special from other control techniques [9]. Moreover, VSI with SMC control requires effective and adaptive switching control reaching law and dynamic sliding surface characterization to ensure voltage regulation with minimum steady state error and reaching time under extreme operating conditions. While achieving these objectives for V2L operation, fast and infinite switching at inverter takes place. The limitations of switching frequency and current inertia associated with VSI leads to major problem along the sliding surface, termed as chattering. In order to avoid chattering without compromising much on robustness and dynamic behavior, numerous worth mentioning efforts have been made, mainly focusing: i) sliding surface design ii) reaching law design.

In [10] Gudey and Gupta proposed fast terminal sliding mode control (FTSMC) for VSI, FTSMC is based on sliding surface using linear and non-linear characteristics. This non-linear surface design based FTSMC reduces the tracking and sliding time but missed the luck to reduced tracking error significantly. Fractional order SMC for distributed energy resource system with black start functionality is proposed in [11] to ensure regulated voltage supply under unbalanced load conditions. However, these objectives are achieved at the cost computational burden and complexity in implementation. In [12] it is shown that fixed value of sliding surface coefficient is a trade-off between tracking time under current disturbances and time consumed by system states to reach sliding surface. In order to handle this trade-off better, various effort have been made to design sliding surface with adjustable sliding surface coefficient [13] & [14]. The concept of rotation of sliding surface technique is proposed in [15], idea of which is derived from 1D and 2D Fuzzy based rules adopted in [16-17], respectively. Komurkugil et al in [18] motivated by the idea of single input fuzzy logic controller (SIFLC) based on state variables to adjust the value of sliding surface coefficient leads to rotating sliding surface mechanism, applied and tested on VSI.

SMC guarantees asymptotic convergence of system states to the sliding surface with convergence time associated with the value of reaching law control gain [19]. Many variants of conventional reaching laws have been addressed in [20] like constant reaching law (C-RL), power rate reaching law(PR-RL), constant hybrid with proportional reaching law. Thus the proficiency of handling trade-off between convergence time, chattering and robustness better, E-RL based SMC are adopted widely in many non-linear systems [21]. In [22], slight modifications to E-RL proved beneficial in achieving reduced chattering with

Preprints (www.preprints.org) | NOT PEER-REVIEWED | Posted: 11 October 2022 doi:10.20944/preprints202210.0143.v1

low total harmonic distortion (%THD). Moreover, E-RL based on Discrete Time Repetitive (DTR) SMC is proposed in [23] for three phase VSI to achieve improved steady state response with reduced chattering. Cos function integrated with power function is used to modify E-RL in [24] to achieve improved convergence rate with evident chattering reduction along the surface. However, restricted control gain magnitude limits the reaching time and chattering reduction capacity. Power Rate Exponential Reaching (PRERL) and Fractional Power Rate Reaching Law (FPRRL) proposed in [25] and [26], respectively. Both reaching laws have succeeded in achieving marginal improvement in reaching time, robustness and chattering reduction.

Therefore, multiple constraints associated with already proposed reaching laws particularly for three phase TLVSI gives enough motivation to develop state of the art reaching law that ensures improved convergence rate, robustness of a system with reduced level of chattering and % THD.

Following which, few of the limitations, necessary to cater are listed below:

- **i.** Most of the scholarly work focuses mainly, one of the two key challenges associated with designing SMC based three phase VSI i-e effective reaching law and appropriate sliding surface.
- **ii.** Value of reaching law gain performs key role in achieving robustness, the large value of reaching law gain serves to achieve higher reaching speed with undesirable chattering along the sliding surface. Similarly, chattering along the surface reduces at lower value of reaching law gain but at the cost of slow reaching speed of system states to the surface. Therefore, this trade-off is critical to handle and extensive high rate scholarly work has been done so far, still, it is call of the day to handle this trade-off in a much better way for sensitive loads.
- **iii.** Robustness of the three phase VSI is guaranteed when system states reaches the sliding surface, however, the dynamic performance and behavior of the inverter is strictly associated with proper selection of the value of sliding coefficient. At smaller value of sliding coefficient, output voltage of the inverter will take more time to track its reference due to slower convergence rate along sliding surface. While at larger value of sliding coefficient, tracking time reduces with increase in reaching time.
- **iv.** Following the severity of above mentioned issues, several effective techniques have been proposed so far. Keeping in view the sensitivity associated with three phase TLVSI for V2L applications, there is still much room of improvement available to achieve high level of robustness with mitigated chattering.

Targeting the abovementioned issues, key contributions of this article are numbered below:

- **i.** A novel reaching law function for setting the value of control gain considering distance of system states from the sliding surface for three phase TLVSI is proposed. Higher value of control gain is set at greater distance to ensure high robustness and convergence rate while value of control gain is lowered following the decreasing distance and it vanishes on the surface to mitigate chattering.

Preprints (www.preprints.org) | NOT PEER-REVIEWED | Posted: 11 October 2022 doi:10.20944/preprints202210.0143.v1

ii. Three phase VSI with SMC based control for V2L applications is designed, comprising rotating sliding surface selection mechanism based on single input fuzzy logic control (SIFLC) and proposed novel composite reaching law.

iii. Behavior of the proposed reaching law based SMC along with PRERL[25], RRL[27] and EERL[22] are tested on different values of gain, for three phase VSI in $\alpha\beta$ stationary frame. It is shown from the comparative analysis that the proposed reaching law performs remarkably well in achieving low reaching time at low value of gain and chattering as well as extremely low reaching time without compromising much on chattering at high value of gain.

iv. The proposed reaching law based SMC, PRERL [25], RRL [27] and EERL [22] are tested on three phase TLVSI under extreme conditions of non-linear load. Results have shown that proposed reaching law has extremely fast transient response with excellent voltage regulation from no load to full-load conditions. Moreover, with fast convergence rate and high degree of robustness, the proposed reaching law offered low %THD and reduced chattering.

2. System Description

To derive critical loads in V2L mode, EVs are equipped with three phase TLVSI [7]. Following which, the proposed control system design with H-bridge circuit topology for three phase VSI is shown in Figure 2. Filter inductor, capacitor and inductor's parasitic resistance is represented as L, C and r , respectively. Input DC voltage from the battery of EV is shown as V_S. Control feedback variables of interest are voltage across capacitor and current through the filter capacitor shown as $V_{c(abc)}$ and $i_{c(abc)}$, respectively. The control scheme of proposed law is designed in stationary (α, β) reference frame.

2.1. System Modeling for Three phase VSI:

Applying energy conservation laws (KVL/KCL) on the circuit shown in Figure 2, following equalities can be deduced:

$$\begin{cases} C\dfrac{dv_{jn}}{dt} = i_{Cj} \;\; ; \;\; j = a,b,c \\ L\dfrac{di_{Lj}}{dt} + ri_{Lj} = u_{j0} - v_{jn} - v_{n0} \;\; ; \;\; v_{n0} = 0 \\ i_{Lj} = i_{Cj} + \dfrac{v_{jn}}{Z_j} \\ v_{j0} = v_{jn} + v_{n0} \\ \sum_{j}^{i_{Lj}} = \sum_{j}^{v_{jn}} = 0 \; ; Energy\ Conservation\ Law \end{cases} \quad (1)$$

Preprints (www.preprints.org) | NOT PEER-REVIEWED | Posted: 11 October 2022 doi:10.20944/preprints202210.0143.v1

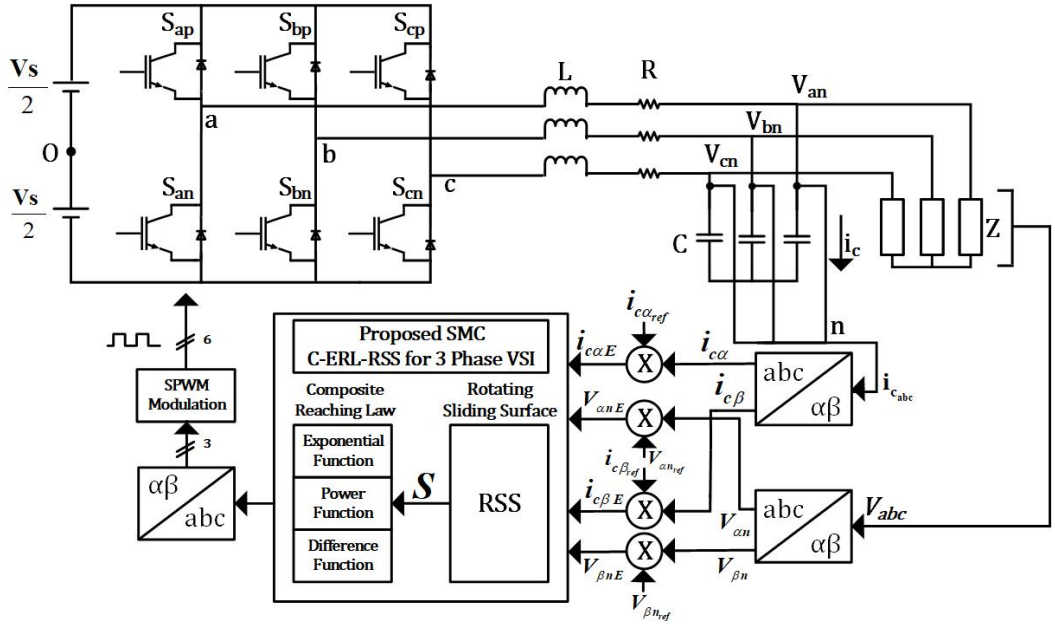

Figure 2. Three Phase VSI with proposed reaching law based SMC.

where, each phase is represented by $j = a, b, c$. Capacitor voltage and current are represented by v_{jn} and i_{Cj}, respectively. In order to decouple abc axes, abc is transformed into stationary $\alpha\beta$ reference frame coordinate system. Following is the $abc{\sim}\alpha\beta$ transformation matrix [19-discrete time repetitive smc] :

$$T_{abc\sim\alpha\beta} = \frac{2}{3}\begin{bmatrix} 1 & -\frac{1}{2} & -\frac{1}{2} \\ 0 & -\frac{\sqrt{3}}{2} & \frac{\sqrt{3}}{2} \end{bmatrix} \qquad (2)$$

The state space equation for three phase VSI with state variables v_{kn} and i_{Ck} in stationary $\alpha\beta$ reference frame can be derived as:

$$\frac{d}{dt}\begin{bmatrix} v_{kn} \\ i_{Ck} \end{bmatrix} = A\begin{bmatrix} v_{kn} \\ i_{Ck} \end{bmatrix} + Bu_k + D \;\; ; \;\; k = \alpha, \beta \qquad (3)$$

where u_k represents the control input and after simplifying (1) matrices A & B are derived as:

$$A = \begin{bmatrix} 0 & \frac{1}{C} \\ -\frac{Z_j + r}{Z_j L} & -\left(\frac{1}{Z_j C} + \frac{r}{L}\right) \end{bmatrix} \quad \text{and} \quad B = \begin{bmatrix} 0 \\ -\frac{V_S}{2L} \end{bmatrix}$$

Representing state variables $\begin{bmatrix} v_{kn} \\ i_{Ck} \end{bmatrix}$ by x, (1) can be simplified as :

$$\dot{x} = Ax + Bu_k + D \qquad (4)$$

The state space model of the system shown in (4) is same for both axes, moreover, following control design is valid to apply on any axes.

3. Sliding Mode Control Design:

Following the characteristics of three phase VSI, capacitor current is the best reflection of change in output voltage. Therefore, selecting capacitor current error and voltage error as

Preprints (www.preprints.org) | NOT PEER-REVIEWED | Posted: 11 October 2022 doi:10.20944/preprints202210.0143.v1

state variables leads to the best control design for output voltage regulation. The voltage error and capacitor current relation can be described as:

$$e = x_{ref} - x = \begin{bmatrix} e_1 \\ e_2 \end{bmatrix} \quad (5)$$

$$e_1 = v_{kref} - v_{kn} \quad (6)$$

$$e_2 = i_{Ckref} - i_{Ck} = \frac{1}{C}\dot{e_1} \quad (7)$$

$$x_{\alpha ref} = \begin{bmatrix} v_{\alpha ref} \\ i_{C\alpha ref} \end{bmatrix} = \begin{bmatrix} V_o \sin(\omega t) \\ \omega V_o \cos(\omega t) \end{bmatrix} \quad (8)$$

$$x_{\beta ref} = \begin{bmatrix} v_{\beta ref} \\ i_{C\beta ref} \end{bmatrix} = \begin{bmatrix} V_o \sin(\omega t - 90^{\circ}) \\ \omega V_o \cos(\omega t - 90^{\circ}) \end{bmatrix} \quad (9)$$

Where V_o is the amplitude of required output voltage and ω is the angular frequency. From (5), (6) and (7), state space form (4) can be represented as:

$$\dot{e} = Ae + Bu_k + D \quad (10)$$

where,

$$D = \begin{bmatrix} 0 \\ C\ddot{v}_{kref} + \frac{\dot{v}_{kref}}{Z_k} + \frac{v_{kref}}{L} \end{bmatrix}$$

Generally, in SMC there are two modes of operations i-e the sliding mode and the reaching mode. In reaching mode, reaching law is applied to force system state to reach the sliding surface quickly. Hence, effective reaching law based on distance of system states from the sliding surface ensures stability, that will be discussed later in the paper. And once the system states are on the sliding surface, system is said to be in sliding mode of operation. Moreover, during sliding mode of operation, robustness is guaranteed and dynamics of the three phase VSI can be determined through (4). An equivalent control law shall be applied to drive the system states along the sliding surface. Specific to the case of three phase VSI, switching frequency constraint leads to the zigzag movement of system states along the sliding surface, that eventually results in chattering. Besides stability and robustness achieved in sliding mode and reaching phase, respectively; steady state and dynamic performance of the system can only be achieved catering both reaching law and sliding surface selection. Thus, both reaching law and sliding surface simultaneously play their role to improve the performance of SMC.

Therefore, in order to design SMC for three phase VSIs, following are the two most important parameters of interest:

3.1. Appropriate sliding surface selection:

Suitable sliding surface selection is one of the most vital concerns to address. Normally, sliding surface is the linear function of state variables and can be represented as:

$$S = [\lambda \quad 1]\begin{bmatrix} e_1 \\ e_2 \end{bmatrix} = Ce \qquad ; \lambda > 0 \quad (11)$$

Where, λ is coefficient of sliding surface .The dynamic behavior of sliding surface (11) in the absence of external disturbances on a surface can be shown as:

$$S_\alpha = \lambda e_{1\alpha} + e_{2\alpha} = \lambda e_{1\alpha} + \dot{e_{1\alpha}} = 0 \quad (12)$$

$$S_\beta = \lambda e_{1\beta} + e_{2\beta} = \lambda e_{1\beta} + \dot{e_{1\beta}} = 0$$

Preprints (www.preprints.org) | NOT PEER-REVIEWED | Posted: 11 October 2022 doi:10.20944/preprints202210.0143.v1

In phase plane $(e_{1\alpha\beta} - e_{2\alpha\beta})$, $S = 0$ represents a sliding line passing through the origin having slope of $-\lambda$.

$$\dot{e_{1\alpha\beta}} = -\lambda e_{1\alpha\beta} \quad (13)$$

First order equation (13) can be solved to express output voltage error as:

$$e_{1\alpha\beta}(t) = e_{1\alpha\beta}(0)e^{-\lambda t} \;\; ; \;\; \lambda > 0 \quad (14)$$

Strictly positive real value of λ ensures asymptotic stability . With this, the significance of λ is well proven. Thus, the optimal value of λ can easily be determined which depends upon the system state variables $\dot{e_{1\alpha\beta}}$ and $e_{1\alpha\beta}$. SIFLC adopted by Komurkugil in [25] for single phase VSI is modified with minor adjustments to make it viable for applying on three phase TLVSI. Thus the following linear function is used to rotate the surface with changing state space variables:

$$\lambda_\alpha{}^R(t) = -0.45E_{d\alpha}(t) + 0.5$$
$$\lambda_\beta{}^R(t) = -0.45E_{d\beta}(t) + 0.5$$

Where,

$\lambda_\alpha{}^R(t)$ and $\lambda_\beta{}^R(t)$ are rotating sliding coeffient for α and β stationary frame, respectively, and

$$E_{d\alpha}(t) = |E_{1\alpha}(t)| - |\dot{E_{2\alpha}}(t)| \;\; ; \;\; E_{1\alpha}(t) = K_1 e_{1\alpha} \wedge E_{2\alpha} = K_2 e_{2\alpha}$$
$$E_{d\beta}(t) = |E_{1\beta}(t)| - |\dot{E_{2\beta}}(t)| \;\; ; E_{1\beta}(t) = K_1 e_{1\beta} \wedge E_{2\beta} = K_2 e_{2\beta}$$

Where, K_1 and K_1 are the scaling gains. Following this eq(12) is modifiefied to rotating sliding surface equation and can be represented as:

$$S_\alpha = \lambda_\alpha{}^R(t)e_{1\alpha} + e_{2\alpha} = 0 \quad (15)$$
$$S_\beta = \lambda_\beta{}^R(t)e_{1\beta} + e_{2\beta} = 0$$

For simplicity, lets take $S = S_{\alpha\beta}$ and from (6) and (7) $e_1 = e_{1\alpha\beta}$, $e_2 = e_{2\alpha\beta}$ and $\lambda = \lambda_{\alpha\beta}{}^R$

Thus (15) can be written as

$$S = \lambda_\beta{}^R(t)e_1 + e_2 = 0$$

3.1.1. Proposed Composite Exponential Reaching Law for Three Phase VSI:

In this section of the paper, mathematical formulation of the proposed composite exponential reaching law for three phase VSI is presented. The proposed reaching law incorporates benefits of the reaching laws referenced in related work section and ensures improved convergence rate than traditional reaching laws. The proposed reaching law is the extension of composite exponential reaching law proposed for single phase VSI in [28].

Stability Analysis: Lyapunov stability function is mentioned below, where S represent $S_{\alpha\beta}$:

$$\dot{V} = S^T \times \dot{S}$$

Hence, the stability condition $\dot{V} < 0$ can be deduced as :

$$\begin{cases} \dot{S} < 0 \;\; if \; S > 0 \\ \dot{S} > 0 \;\; if \;\; S < 0 \end{cases}$$

First derivative of (11) can be shown as:

$$\dot{S} = C\dot{e} \quad (15)$$

From (10) and (15), the control law can be represented as:

$$u_k = -(\dot{S} + CAe + CD)(CB^{-1}) \quad (16)$$

Preprints (www.preprints.org) | NOT PEER-REVIEWED | Posted: 11 October 2022 doi:10.20944/preprints202210.0143.v1

The reaching law is mathematically termed as rate of change of sliding surface. Thus the reachability principal and its significance in control input can easily be visualize.
The proposed composite exponential reaching law(C-ERL) for three phase VSI is given as:

$$\dot{S} = \left[|S|\left(\mu + (1-\mu)e^{-\gamma|S|^{\delta}}\right) - \frac{M|S|}{\mu+(1-\mu)e^{-\gamma|S|^{\delta}}\cos(\varepsilon|S|)}\right] sign(S) \qquad (17)$$

Where $0 < \mu < 1, \gamma > 0, \delta > 0, M > 0 \; and \; \varepsilon > 0$
Level of adaptability and effective nature of the proposed reaching law in (17) can be verified under following conditions:

i) $\boldsymbol{S \gg 0}$ **:** If system states are far away from the sliding surface, very high value of gain will be set to ensure fast convergence of system states to the stable surface $S = 0$.

ii) $\boldsymbol{S \approx 0}$ **:** If system states are near to the sliding surface, $\mu + (1-\mu)e^{-\gamma|S|^{\delta}}\cos(\varepsilon|S|) \approx 0$ that leads to $\frac{M|S|}{\mu+(1-\mu)e^{-\gamma|S|^{\delta}}\cos(\varepsilon|S|)} < 1$ and $|S|\left(\mu + (1-\mu)e^{-\gamma|S|^{\delta}}\right) < \frac{M|S|}{\mu+(1-\mu)e^{-\gamma|S|^{\delta}}\cos(\varepsilon|S|)}$; thus the value of overall gain set will be negligible. Thus mitigating chattering along the sliding surface.

iii) $\boldsymbol{S \to 0}$ **:** The values of $\mu, \gamma, \delta \; and \; \varepsilon$ are set in a way that value of reaching law gain becomes directly proportional to the distance of system states from reference sliding surface $S = 0$ .Assume if $e^{-\gamma|S|^{\delta}}\cos(\varepsilon|S|) \approx 0$ then $\mu + (1-\mu)e^{-\gamma|S|^{\delta}}\cos(\varepsilon|S|) \approx \mu < 1$ that eventually results in higher value of $\frac{M|S|}{\mu+(1-\mu)e^{-\gamma|S|^{\delta}}\cos(\varepsilon|S|)}$. Where as $|S|\left(\mu + (1-\mu)e^{-\gamma|S|^{\delta}}\right) < \frac{M|S|}{\mu+(1-\mu)e^{-\gamma|S|^{\delta}}\cos(\varepsilon|S|)}$, therefore the value of reaching law gain is adjusting based on distance of system states from $S = 0$.

Thus, the value of reaching law control gain set by proposed reaching law for three phase VSI adopts the most efficient convergence mechanism to force system states to the reference surface in finite time. From [33] , $e^{-\gamma|S|^{\delta}}cos(\varepsilon|S|)$ is tailored with the proposed reaching law to achieve fast damping characteristics along the surface and force system states to coincide asymptotically to the equilibrium surface. Furthermore, $|S|\left(\mu + (1-\mu)e^{-\gamma|S|^{\delta}}\right)$ in the reaching law serves to adjust and mitigate gain value near the equilibrium surface to ensure extreme possible chattering reduction along the sliding surface.

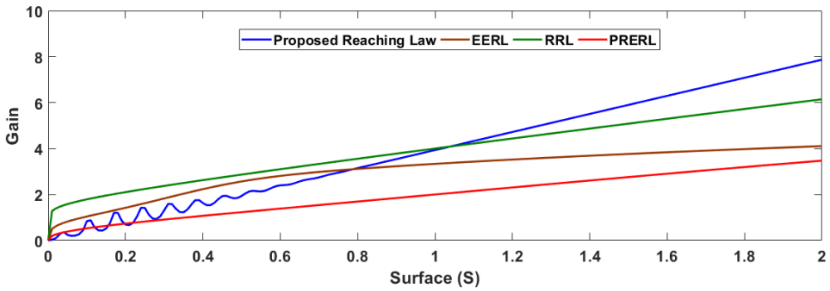

Figure 3. Reaching law Gain adaptive behavior w.r.t distance of surface from equilibrium point.

Preprints (www.preprints.org) | NOT PEER-REVIEWED | Posted: 11 October 2022 doi:10.20944/preprints202210.0143.v1

Adoptability behavior for setting reaching law control gain value with reference to the distance of system states from the equilibrium surface is shown in Figure 3. That shows comparative analysis of the behavior of state of the art and latest reaching laws like enhanced exponential reaching (EERL)[22], repetitive reaching law (RRL)[27], power rate exponential reaching law(PRERL)[25] and proposed composite exponential reaching law with rotating sliding surface(C-ERL-RSS). The parametric values of reaching law variables used in analysis are mentioned in Table I.

At distance $S = 2$ far from the equilibrium point $S = 0$, the reaching law is supposed to set the higher value of gain to ensure fast convergence rate to achieve shorter reaching time. It is evident from the Figure 3, that proposed reaching law sets the highest gain value at $S = 2$ i-e $Gain = 8$, thus, ensuring fast convergence rate to achieve shorter reaching time. Moreover, the reaching law must be capable of adjusting gain value as the surface approaches towards the equilibrium point $S = 0$. The reaching law control gain value must be lowered as surface approaches $S = 0$, following this condition all reaching laws successfully fulfill this criteria. The reaching law control gain value of proposed C-ERL-RSS got lowered from RRL ,EERL and PRERL at $S = 1.1$, $S = 0.8$ and $S = 0.1$, respectively.

Table I. Parametric values of reaching laws.

	Reaching Law	Parametric Values
EERL[22]	$\dot{S} = \left[-KS - \frac{M\lvert S\rvert}{\mu + (1-\mu)e^{-\gamma\lvert S\rvert^{\delta}}}\right] sign(S)$	$\gamma = 10, \delta = 2, K = 10$ $\mu = 0.6, \quad M = 2$
RRL[27]	$\dot{S} = [-KS - M\lvert S\rvert^{\tau}] sign(S)$	$K = 10, M = 2, \tau = 0.3$
PRERL[25]	$\dot{S} = \left[-\frac{M\lvert S\rvert^{\tau}}{\mu + (1-\mu)e^{-\gamma\lvert S\rvert^{\delta}}}\right] sign(S)$	$\gamma = 10, \delta = 2, \tau = 0.3$ $\mu = 0.6, \quad M = 2$
Proposed C-ERL-RSS	$\dot{S} = \left[\lvert S\rvert \left(\mu + (1-\mu)e^{-\gamma\lvert S\rvert^{\delta}}\right) - \frac{M\lvert S\rvert}{\mu + (1-\mu)e^{-\gamma\lvert S\rvert^{\delta}}\cos(\varepsilon\lvert S\rvert)}\right] sign(S)$	$\gamma = 10, \delta = 2, \varepsilon = 85$ $\mu = 0.6, \quad M = 2$

However, very near to the equilibrium point $S \approx 0$, the reaching law control gain must diminish to overcome chattering curse along the sliding surface $S = 0$. It can be easily observed from the Figure 2 that the value of the proposed C-ERL-RSS reaching law control gain is got lowered compared to other reaching law values that almost vanished at $S \approx 0$. Therefore, it is obvious to conclude from the above discussion that the desired adoptive behavior for setting reaching law control gain value is effectively fulfilled by the proposed C-ERL-RSS. The comparative analysis of proposed C-ERL-RSS with other reaching laws shown in Figure 3 is tabulated in Table II.

Table II. Reaching Law behavior interms of reaching time and chattering.

Reaching Law	Reaching Time	Chattering
EERL[22]	High	Moderate
RRL[27]	Moderate	High
PRERL[25]	High	Low
Proposed C-ERL-RSS	Low	Low

Preprints (www.preprints.org) | NOT PEER-REVIEWED | Posted: 11 October 2022 doi:10.20944/preprints202210.0143.v1

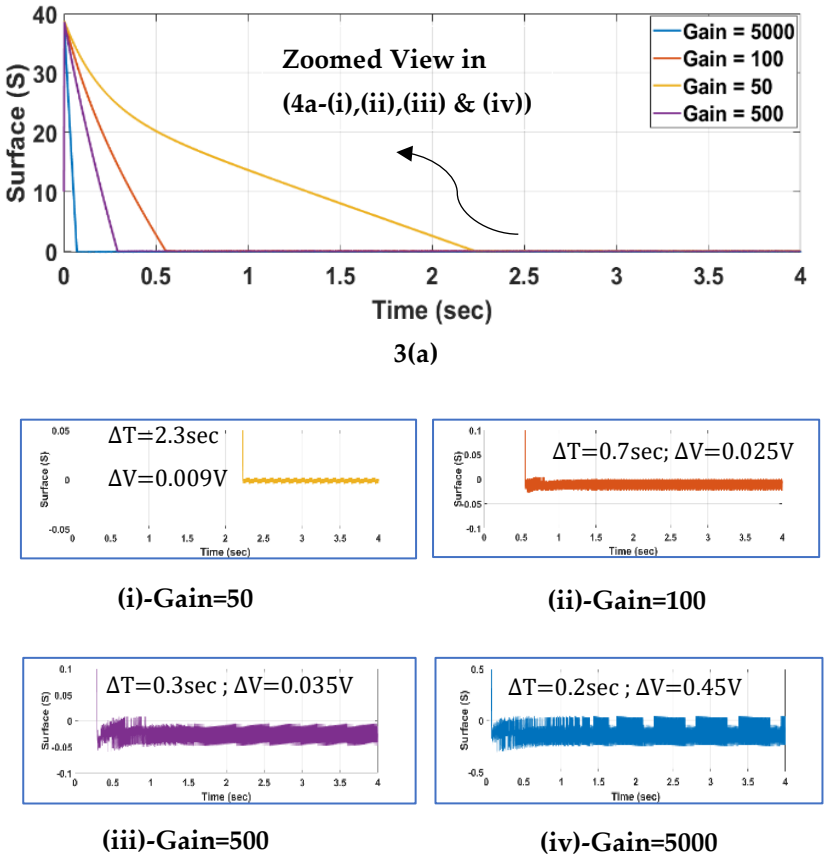

Figure 4(a).PRERL-Reaching Law behavior at differen gain values .Zoomed view to analyse chattering and reaching time at 50, 100, 500 and 5000 gain values at (i),(ii),(iii) and (iv) respectively.

The proposed reaching law along with other state-of-the art reaching laws are implemented on the state space model of three phase TLVSI in stationary $\alpha\beta$ reference frame shown in (4) , the comparative analysis of the performance of proposed reaching law with other well-known reaching laws, on the basis of reaching time and chattering at different reaching law gain values is presented in Figure 4(a) to Figure 4(d).

It is quite evident from Figure.4(a) and 4(b) that at lower value of reaching law gain (Gain=50) , the unwanted chattering along the sliding surface is negligible i-e 0.009v and 0.1v, respectively. While reduction in chattering at such a low level is at the cost of very high reaching time of 2.3sec and 2.2sec for PRERL and RRL, respectively. However, the problem of high reaching time is handled better applying higher gain values i-e reaching time at 100, 500 and 5000 are witnessed as 0.7sec, 0.3sec and 0.2sec for PRERL and 0.45sec, 0.25sec and 0.18sec for RRL, respectively.The performanceof reaching law is measured based on reduced reaching time and chattering simultaneously at different values of gain. Therefore, the chattering of PRERL at gain=100, gein=500 and gain=5000 is observed as 0.025v, 0.035v and 0.45v, respectively.Likewise, the chattering magnitude of RRL at gain=100, gain=500 and gain=5000 is measured as 0.015v, 0.045v and 0.25v respectively. Thus performance of PRERL and RRL is a much compromise option between reaching time and chattering.As far as V2L application is concerned, fast transient response with minimal chattering along the surface is necessary to derive critical loads.

Preprints (www.preprints.org) | NOT PEER-REVIEWED | Posted: 11 October 2022 doi:10.20944/preprints202210.0143.v1

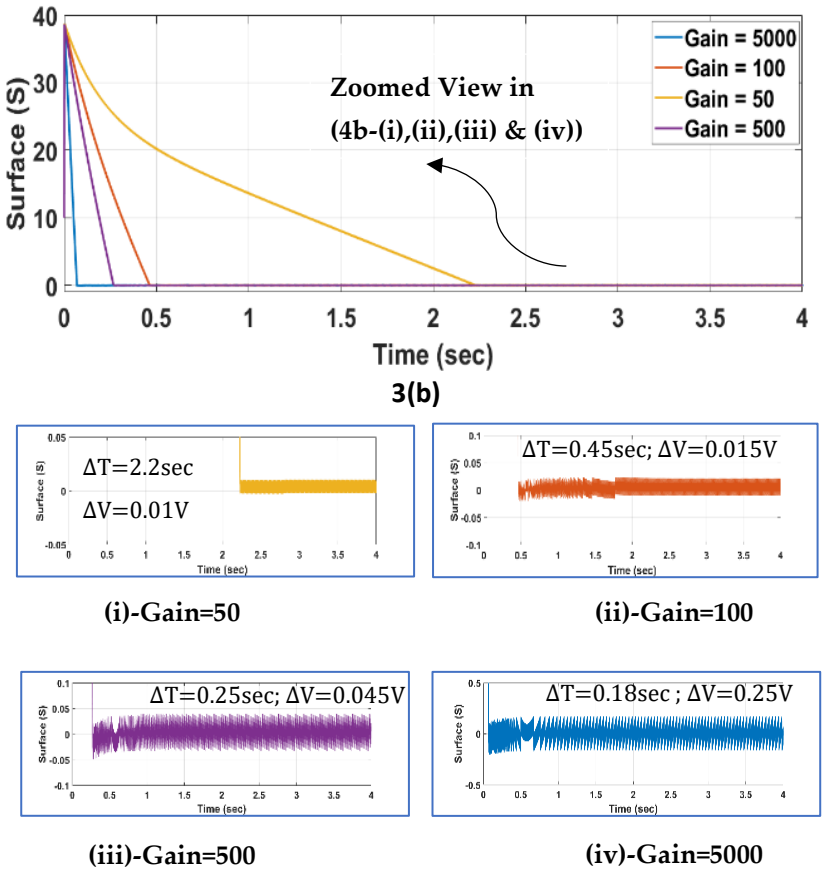

Figure 4(b): RRL-Reaching Law behavior at differen gain values . Zoomed view to analyse chattering and reaching time at 50, 100, 500 and 5000 gain values at (i),(ii),(iii) and (iv), respectively.

Thus , the bahvior of PRERL and RRL clearly shows that their performance is more or less similar in nature. One of the two desired benefits i-e reduced reaching time and mitigated chattering long the sliding surface can be achieved at specific value of gain. High reaching time , low chattering at higher values of gain and low reaching time with higher chattering magnitude.Moreover, if the adaptivr nature of reaching law is considered, still this behavior of performance leads to very low transient response ans well as setling time.Also, the reaching law gain value cannot be mittigated to the desired level necessary to handle critical loads.

Preprints (www.preprints.org) | NOT PEER-REVIEWED | Posted: 11 October 2022 doi:10.20944/preprints202210.0143.v1

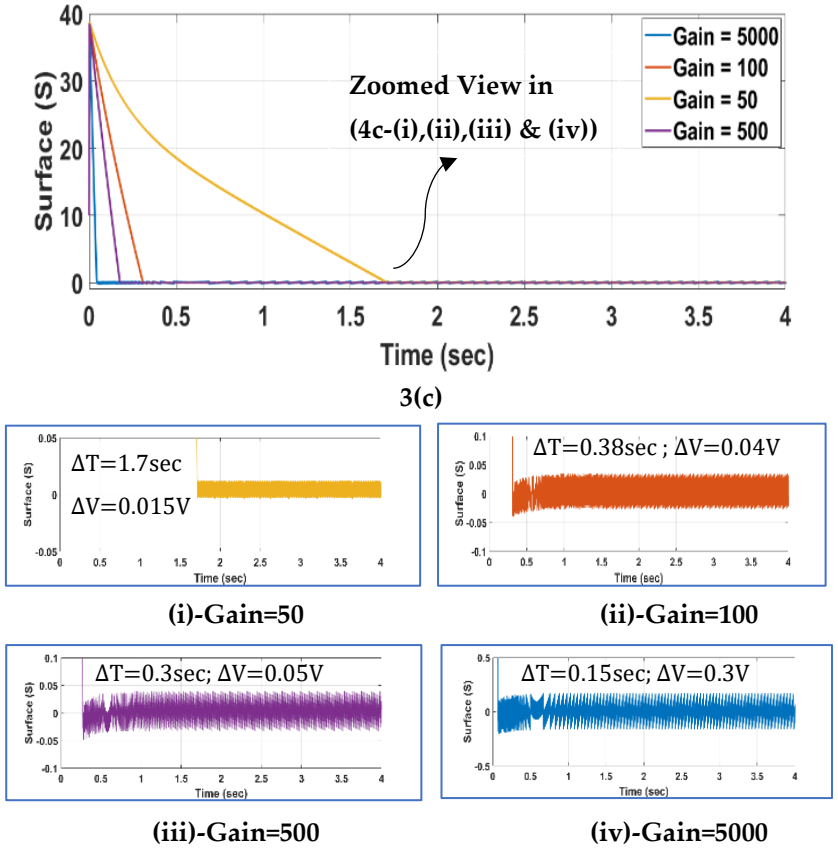

Figure 4(c): EERL-Reaching Law behavior at differen gain values .Zoomed view to analyse chattering and reaching time at 50, 100, 500 and 5000 gain values at (i),(ii),(iii) and (iv), respectively.

To some extent, the problem of high reaching time at lower gain value of 50 is solved by EERL while maintaining smaller chattering magnitude, as shown in Figure 4(c). The reaching time is reduced to 1.7sec with chattering of 0.015v along the surface. Moreover, this improvement in behavior is also witnessed at higher values of gain i-e 100, 500 and 5000. The reaching time and chattering magnitude observed at 100, 500 and 5000 are 0.38sec, 0.3sec, 0.15sec and 0.04v, 0.05v, 0.3v, respectively.

The performance of proposed reaching law under different gain values is shown in Figure 4(d). In order to achieve reduced reaching time under low value of gain (Gain=50), the proposed reaching law has proven to be the most effective among other reaching laws, while maintain low level of chattering along the sliding surface. The response shown in Figure 4(d) is further highlighted as zoomed view in Figure.3(d)-i for Gain=50, the reduced reaching time with minimal possible chattering level is found to be 0.7sec and 0.01v. Moreover, this encouraging behavior continuous even at higher values of gain, i-e at Gain=100, the reaching time is found to be 0.3sec with chattering of 0.03v along the surface, at Gain=500 and Gain=5000, reaching time and chattering is observed as 0.2sec, 0.05sec and 0.05v,0.3v , respectively.

Preprints (www.preprints.org) | NOT PEER-REVIEWED | Posted: 11 October 2022 doi:10.20944/preprints202210.0143.v1

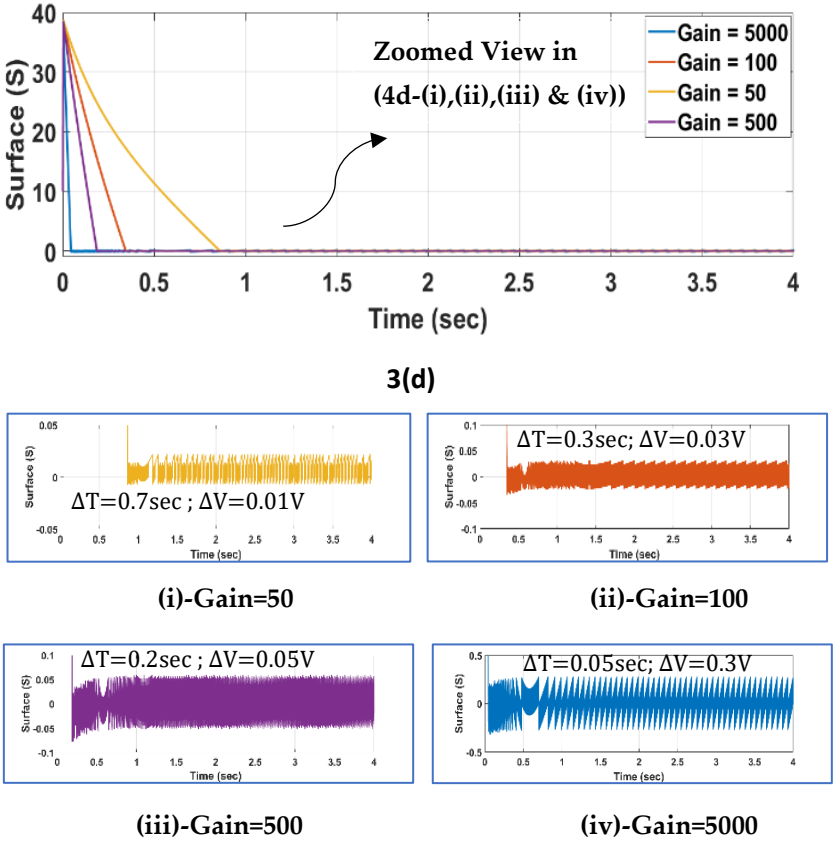

Figure 4(d):Proposed C-ERL-RSS-Reaching Law for three phase VSI behavior at differen gain values .Zoomed view to analyse chattering and reaching time at 50, 100,500 and 5000 gain values at (i),(ii),(iii) and (iv), respectively.

It is worth mentioning here that at higher values of gain i-e 5000, the chattering magnitude of RRL, EERL and proposed reaching law are very near to each other. Thus, the important factor to notice here is the outstanding reduction in reaching time of 0.05sec as compared to other reaching laws, while ensuring either very little or same chattering level. Therefore, one can easily visualize the adaptive and effective nature of proposed reaching law at different gain values to achieve reduced reaching time with minimum possible chattering level.

Following the behavior of reaching laws shown in Figure 4, the relationship between chattering and reaching time at different values of gain is presented in Figure 5. Tremendous reduction in reaching time at low value of gain(Gain=50) is achieved through proposed reaching law while maintaining low level of chattering. Similarly if we follow the trend down on reaching time axis, the reaching time reduction behavior is highly reduced to 0.05sec while ensuring minimum possible level of chattering. Likewise, incase of Gain=100 and Gain=500 this reduction pattern of reaching time continuous with slight increase in chattering as well. At Gain=100, reaching time is observed as 0.3sec with the chattering magnitude of 0.03V, and at Gain=500 , the value of reaching time is reduced to

Preprints (www.preprints.org) | NOT PEER-REVIEWED | Posted: 11 October 2022 doi:10.20944/preprints202210.0143.v1

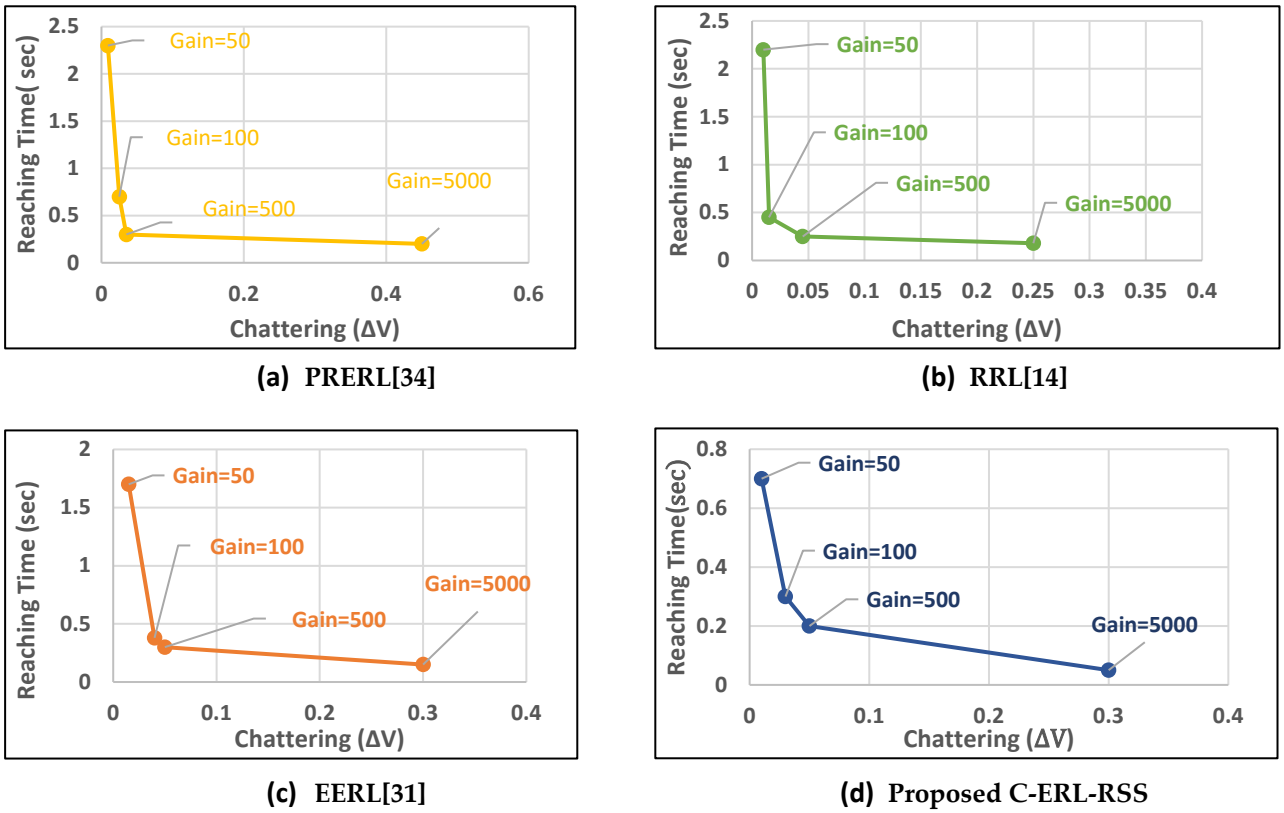

Figure 5. Trade-off between Reaching Time and Chattering on different Gain values: (a) PRERL[25], (b) RRL[27], (c) EERL[22], (d) Proposed C-ERL-RSS

0.02sec with 0.05V of chattering magnitude along the sliding surface. While analyzing the behavior at the higher extreme value of Gain i-e 5000, reaching time is found to be extremely low at 0.03sec with restricted chattering magnitude of 0.03V. Concluding this, if sensitive system major concern is the switches performance at high frequencies i-e reduced chattering, the proposed reaching law at lower value of Gain solves the task with providing extremely low chattering while ensuring fast convergence time as well. On the other hand, PRERL [25], RRL [27] and EERL [22] offer low magnitude of chattering but at the cost of very high reaching time.

4. SMC with Proposed Reaching Law

Relation of first derivative of sliding surface, shown in (15) can also be represented as:

$$\dot{S} = \dot{e_1}\lambda + \dot{e_2} = \dot{e_1}\lambda + \ddot{e_1}$$

Using (10)

$$\dot{S} = \dot{e_1}K - \frac{(r+Z)}{ZL}e_1 - \left(\frac{1}{ZC} + \frac{r}{L}\right)e_2 - \frac{V_s}{2L}u_k \qquad (18)$$

Equating equation (17) and (18)

$$\left[|S|\left(\mu + (1-\mu)e^{-\gamma|S|^{\delta}}\right) - \frac{M|S|}{\mu+(1-\mu)e^{-\gamma|S|^{\delta}}\cos(\varepsilon|S|)}\right] sign(S) = \dot{e_1}\lambda - \frac{(r+Z)}{ZL}e_1 - \left(\frac{1}{ZC} + \frac{r}{L}\right)e_2 - \frac{V_s}{2L}u_k$$

$$u_k = -\frac{2L}{V_s}\left(\left[|S|\left(\mu + (1-\mu)e^{-\gamma|S|^{\delta}}\right) - \frac{M|S|}{\mu+(1-\mu)e^{-\gamma|S|^{\delta}}\cos(\varepsilon|S|)}\right] sign(S) - \dot{e_1}\lambda + \frac{(r+Z)}{ZL}e_1 + \left(\frac{1}{ZC} + \frac{r}{L}\right)e_2\right)$$

For control input for $\alpha\beta$ stationary frame can be segregated in (19) and (20)

Preprints (www.preprints.org) | NOT PEER-REVIEWED | Posted: 11 October 2022 doi:10.20944/preprints202210.0143.v1

$$u_\alpha = -\frac{2L}{V_s}\left(\left[|S|\left((\mu+(1-\mu))e^{-\gamma|S|^\delta}\right) - \frac{M|S|}{(\mu+(1-\mu))e^{-\gamma|S|^\delta}\cos(\varepsilon|S|)}\right] sign(S) - \dot{e}_{1\alpha}\lambda + \frac{(r+Z)}{ZL}e_{1\alpha} + \left(\frac{1}{ZC}+\frac{r}{L}\right)\frac{\dot{e}_{1\alpha}}{C}\right) \quad (19)$$

$$u_\beta = -\frac{2L}{V_s}\left(\left[|S|\left((\mu+(1-\mu))e^{-\gamma|S|^\delta}\right) - \frac{M|S|}{(\mu+(1-\mu))e^{-\gamma|S|^\delta}\cos(\varepsilon|S|)}\right] sign(S) - \dot{e}_{1\beta}\lambda + \frac{(r+Z)}{ZL}e_{1\beta} + \left(\frac{1}{ZC}+\frac{r}{L}\right)\frac{\dot{e}_{1\beta}}{C}\right) \quad (20)$$

4.1. Simulation Study:

In this part of the article, reference tracking trajectory of output voltage for RRL[27], PRERL[25],EERL[22] and proposed reaching law is shown through implementation of three phase TLVSI in MATLAB/Simulink . The performance of aforementioned reaching laws along with proposed reaching law is tested on three phase TLVSI under non-linear rectifier load of 1KW. In figure 6(a) and figure 6(b) refernce tracking trajectory of output voltage and current response, respectively, from no load to full load condition at 0.025sec. It is evident from figure 6(a) that at output voltage starts to track the reference voltage at 4ms under no load condition.Moreover, there is compromised voltage regulation beyond 4ms.Similary, transient time is observed as 3.5ms when load is applied at 0.025ms.

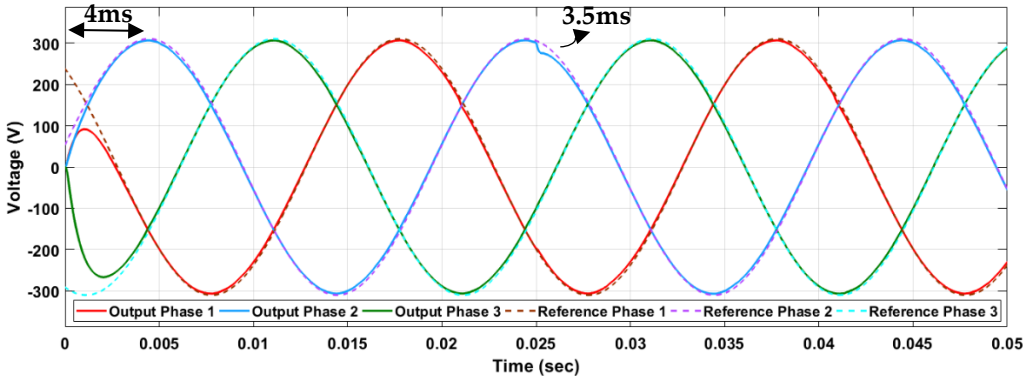

Figure 6(a) :PRERL[25], Output voltage-Reference tracking trajectory and voltage regultaion.

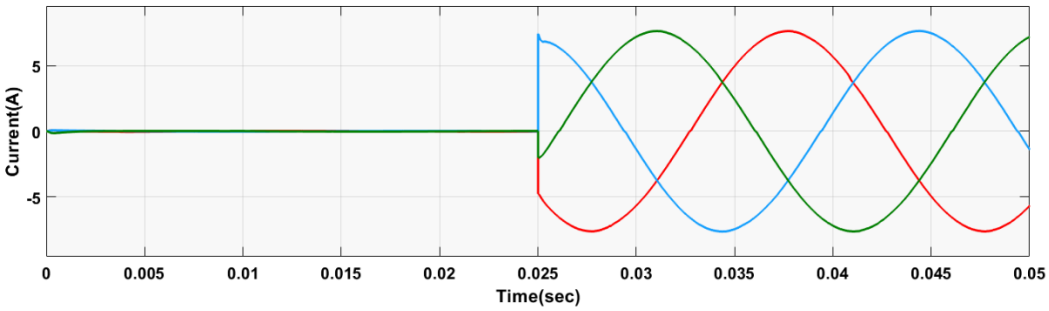

Figure (6b) :PRERL[25], Load current-Step response under extreme load variation.

Likewise, the performance of RRL[27] based SMC under aforementioned conditions is shown in figure 7(a) and figure 7(b).Reference tracking time under no load condition is not much encouraging as output starts following reference voltage at 7msec with more compromised voltage regulation and comparitively slow transient response of 5msec.

Preprints (www.preprints.org) | NOT PEER-REVIEWED | Posted: 11 October 2022 doi:10.20944/preprints202210.0143.v1

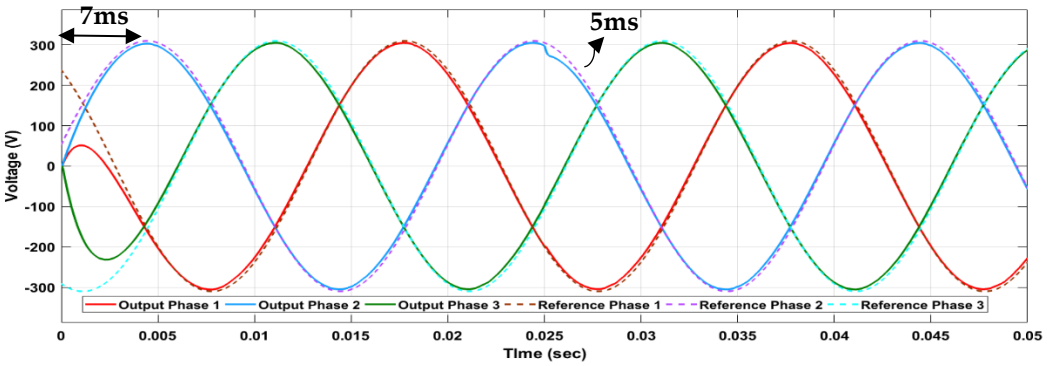

Figure 7(a) :RRL[27], Output voltage-Reference tracking trajectory and voltage regultaion.

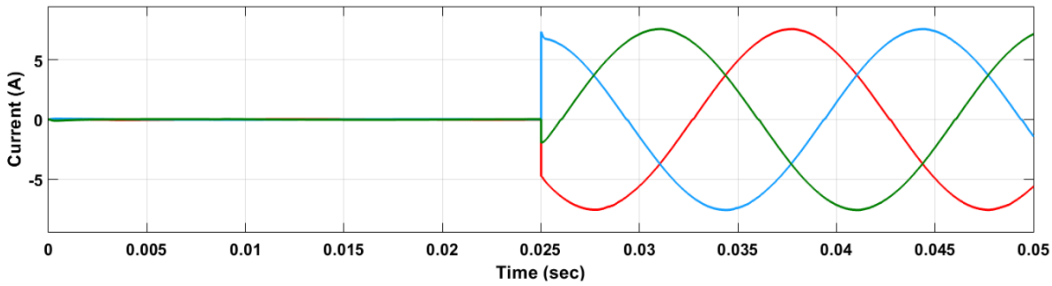

Figure (7b) :RRL[27], Load current-Step response under extreme load variation.

However, the response of EER[22] based SMC, shown in figure(a) and figure (8b) is quite encouraging interms of reduced refernce tracking time under no load condition as well as fast transient response is observed. In figure 8(a) reference tracking is observed and transient time is observed as 2.5ms and 2ms, respectively.Also, better reference voltage tracking leads to improved voltage regulation as compared to RRL[27] and PRERL[34].

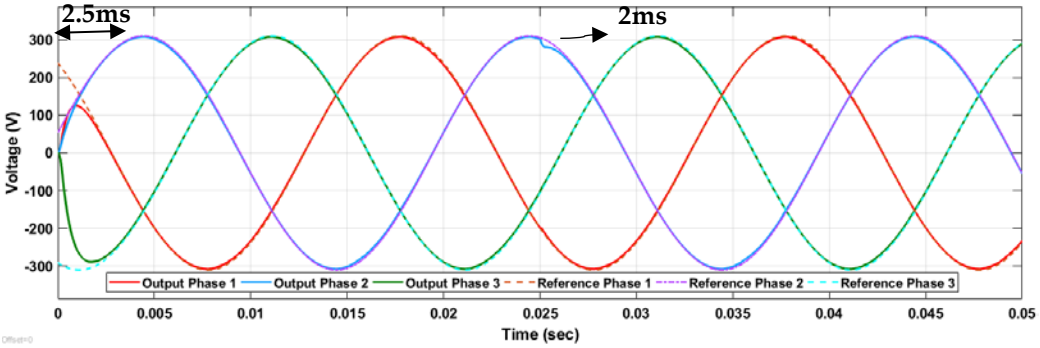

Figure 8(a) :EERL[22], Output voltage-Reference tracking trajectory and voltage regultaion.

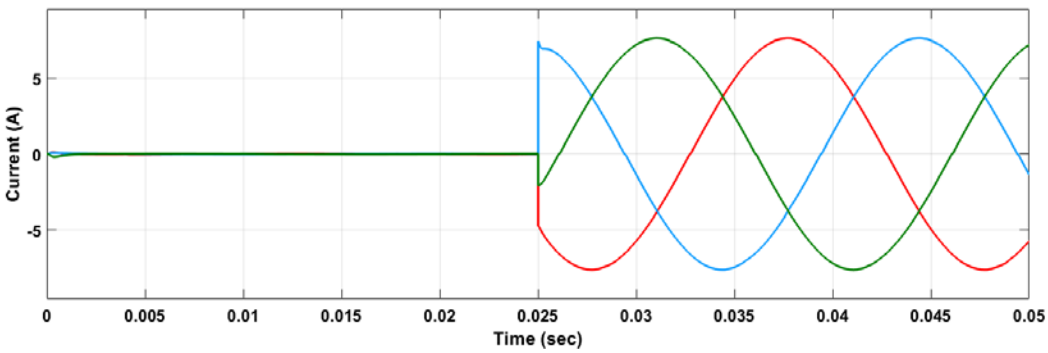

Figure (8b) :EERL[22], Load current-Step response under extreme load variation.

Preprints (www.preprints.org) | NOT PEER-REVIEWED | Posted: 11 October 2022 doi:10.20944/preprints202210.0143.v1

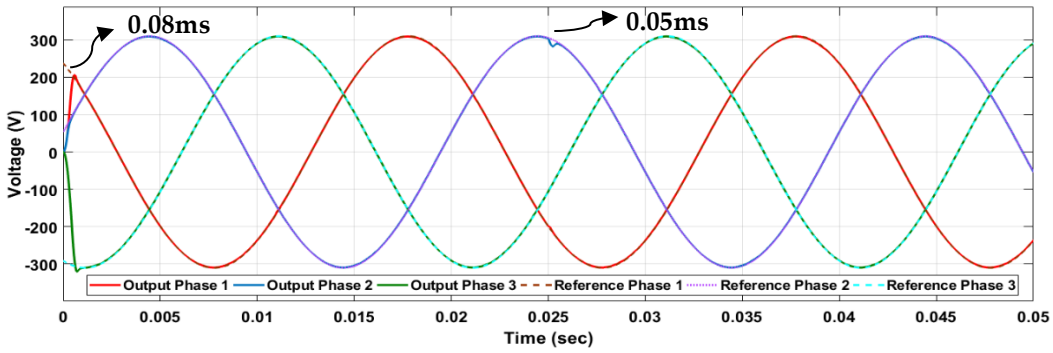

Figure 9(a) : Proposed C-ERL-RSS, Output voltage-Reference tracking trajectory and voltage regultaion.

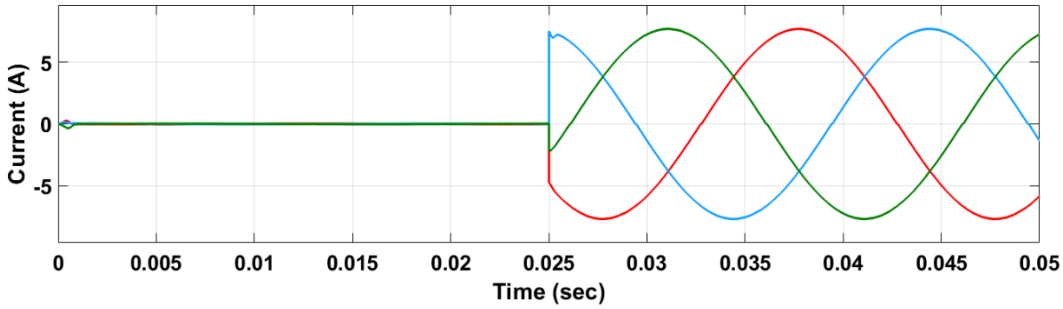

Figure (9b) : Proposed C-ERL-RSS, Load current-Step response under extreme load variation.

The performance of proposed composite reaching law based SMC under predefined conditions for voltage regulation and trajectory tracking is shown in in figure (9).Enormous reduction is reference traccking time of 0.08ms is achieved with extremely fast transient response of 0.05ms at 0.025sec. Tremendous improvent in voltage regulation under no load and full load condions is observed with extremely low %THD of 1.1%. Therefore, the proposed reaching law based SMC has shown remarkable results to make it the most viable option to be used in EVs for V2L applications for handling critical loads.

Table III: Circuit Specifications.

Circuit Parameters	Value
Input DC Voltage from Battery, V_S	500V
Reference Voltage, V_{RMS}	220V
Filter Inductor, L	$4mH$
Filter Capacitor, C	$30\mu F$
Scaling Gain, K_1	$2x10^{-3}$
Scaling Gain, K_2	$2.4x10^{-5}$
Non-Linear Rectifier Load	1Kw
Switching Frequency, f_s [14]	9kHz
Fundamental Frequenct, f	50Hz

The comparative analysis summary of results obtained through implementation of PRERL[25], RRL[14], EERL[22] and proposed composite reaching law along with other state of the art reaching laws based SMC's results obtained from similar system are shown in Table-IV. It can be deduced from the below shown finding of Table-IV that the

Preprints (www.preprints.org) | NOT PEER-REVIEWED | Posted: 11 October 2022 doi:10.20944/preprints202210.0143.v1

proposed composite reaching law based SMC has extremely resiliant behavior against sudden load variations. Moreover, phenomenal reduction in %THD with high level of voltage regulation makes proposed compasite reaching law the best among other reaching laws.

Table IV: Comparison of proposed composite reaching law with other state-of-the art reaching laws

Controller	SMC [37]	DSMC [38]	TSMC [39]	PRERL[25] Compared in this Paper	RRL[27] Compared in this paper	EERL[22] Compared in this paper	Proposed C-ERL-RSS
Input- V_{DC}(V)	360	250	250	500	500	500	500
Reference- V_{RMS}(V)	220	110	110	220	220	220	220
Output-V_{RMS}(V)	-	-	-	218	217	218.4	219.63
$f_{switching}(KHz)$	15	10	20	09	09	09	09
%THD	1.7%	1.6%	5.1%	2.3%	3.2%	1.8%	1.1%
%Voltage Regulation	-	-	-	99.09%	98.63%	99.27%	99.83%
Robustness	-	-	-	Good	Good	Better	Best
Tracking Time(ms)	-	-	-	4	7	2.5	0.08
Transient Time(ms)	0.5	2	2	3.5	5	2	0.05

The event-driven tools are beneficial in terms of the computational effective-ness, processing activity and power consumption reduction and real-time compression [29]-[32]. The feasibility of incorporating these tools in the suggested method can be investigated in future.

5. Conclusion:

A novel composite reaching law based SMC is introduced for three phase TLVSI to derive critical loads in V2L applications. The proposed composite reaching law based SMC has made EVs more reliable in V2L mode of operation to achieve high level of robustness and fast convergence rate under variable load conditions. The comparative analysis advocates that the proposed composite reaching law has the wise mechanism of adjusting gain values to achieve fast convergence rate with reduced chattering even at equilibrium point. The main concept of the proposed reaching law is to set the values of gain based on distance of state variable from the equilibrium surface i-e the gain value must be higher when state variables are far away from the equilibrium surface, similarly gain value must reduce as system states approaches the equilibrium point. Moreover, very near to the surface the gain value must diminishes to eliminate chattering. Following which, an intelligent mix of difference, power and exponential functions is introduced design proposed composite reaching law. In addition to this, SIFLC is used for the selection of optimal rotating sliding surface. The concept of which is based on linear combination of system state variables. The performance of the proposed reaching law for three phase TLVSI authenticates that the proposed reaching law has offered well regulated output voltage with 1.1%THD, better dynamic response and reduced chattering.

Author Contributions: Conceptualization, F.H., M.A., A.W., and S.M.Q.; methodology, F.H., M.A., and A.W.; implementation, F.H. and M.A.; validation, F.H., M.A., A.W., and S.M.Q.; formal analysis, F.H., M.A., and S.U.A.; investigation, F.H., M. A., A.W., and S.M.Q; resources, A.W., S.M.Q., and A.A.; writing—original draft preparation, F.H, M.A., and A.W.; writing—review and editing, S.M.Q., S.U.A., and A.T.A.; visualization, F.H., and M. A.; supervision, M.A., A.W., S.M.Q., and A.T.A.; project administration, A.W., S.M.Q., and A.T.A.; funding acquisition, S.M.Q., and A.T.A. All authors have read and agreed to the published version of the manuscript.

Funding: The authors would like to thank the Effat University for funding this work under the research grant number (UC#9/2June2021/7.2-21(3)5).

Institutional Review Board Statement: Not Applicable.

Informed Consent Statement: Not Applicable.

Data Availability Statement: In this section, please provide details regarding where data supporting reported results can be found, including links to publicly archived datasets analyzed or generated during the study. Please refer to suggested Data Availability Statements in section "MDPI Research Data Policies" at https://www.mdpi.com/ethics. You might choose to exclude this statement if the study did not report any data.

Acknowledgments: The authors are grateful to Bahria School of Engineering and Applied Sciences, Bahria University Islamabad and Effat University, Jeddah, Saudi Arabia for technical support. The authors also acknowledge financial support from the Supply Chain Management Department of the Effat University and from the Electrical and Computer Engineering Department of the Effat University under the grant number (UC#9/2June2021/7.2-21(3)5), Effat University, Jeddah, Saudi Arabia.

Conflicts of Interest: The authors declare no conflict of interest.

References

1. Barja-Martinez S, Rücker F, Aragüés-Peñalba M, Villafafila-Robles R, MunnéCollado n, Lloret-Gallego P. A novel hybrid home energy management system considering electricity cost and greenhouse gas emissions minimization. IEEE Trans Ind Appl 2021;57(3):2782–90. http://dx.doi.org/10.1109/TIA.2021. 3057014
2. Kanellos FD, Grigoroudis E, Hope C, Kouikoglou VS, Phillis YA. Optimal GHG emission abatement and aggregate economic damages of global warming. IEEE Syst J 2017;11(4):2784–93.
3. Houghton J. Global warming the complete briefing, 20097.
4. Yuan J, Dorn-Gomba L, Callegaro AD, Reimers J, Emadi A. A review of bidirectional on-board chargers for electric vehicles. IEEE Access 2021;9:51501–18. http://dx.doi.org/10.1109/ACCESS.2021.3069448.
5. Islam, Shirazul, Atif Iqbal, Mousa Marzband, Irfan Khan, and Abdullah MAB Al-Wahedi. "State-of-the-art vehicle-to-everything mode of operation of electric vehicles and its future perspectives." Renewable and Sustainable Energy Reviews 166 (2022): 112574.
6. M. Curkovic, K. Jezernik, and R. Horvat, ''FPGA-based predictive sliding mode controller of a three-phase inverter,'' IEEE Trans. Ind. Electron., vol. 60, no. 2, pp. 637–644, Feb. 2013.
7. Sayed, Khairy, Abdulaziz Almutairi, Naif Albagami, Omar Alrumayh, Ahmed G. Abo-Khalil, and Hedra Saleeb. "A review of DC-AC converters for electric vehicle applications." Energies 15, no. 3 (2022): 1241.
8. Hasan, M.; Mekhilef, S.; Ahmed, M. Three-phase hybrid multilevel inverter with less power electronic components using space vector. IET Power Electron. 2014, 7, 1256–1265
9. S. J. Chiang, T. L. Tai, and T. S. Lee, ''Variable structure control of UPS inverters,'' IEE Proc.-Electr. Power Appl., vol. 145, no. 6, pp. 559–567, 1998.
10. S. K. Gudey and R. Gupta, "Recursive fast terminal sliding mode control in voltage source inverter for a low-voltage microgrid system," IET Generat., Transmiss. Distrib., vol. 10, no. 7, pp. 1536–1543, 2016.
11. T.-L. Tai and J.-S. Chen, "UPS inverter design using discrete-time sliding-mode control scheme," IEEE Trans. Ind. Electron., vol. 49, no. 1, pp. 67–75, Feb. 2002
12. B. Iliev and I. Hristozov, "Variable structure control using Takagi–Sugeno fuzzy system as a sliding surface," in Proc. IEEE Int. Conf. FUZZ-IEEE, Honolulu, HI, 2002, pp. 644–649.
13. S.-B. Choi, D.-W. Park, and S. Jayasuriya, ''A time-varying sliding surface for fast and robust tracking control of second-order uncertain systems,'' Automatica, vol. 30, no. 5, pp. 899–904, May 1994.
14. A. Bartoszewicz, ''A comment on A time-varying sliding surface for fast and robust tracking control of second-order uncertain systems,'' Automatica, vol. 31, no. 12, pp. 1893–1895, Dec. 1995.
15. A. Šabanovic, ''Variable structure systems with sliding modes in motion control—A survey,'' IEEE Trans. Ind. Informat., vol. 7, no. 2, pp. 212–223, May 2011.
16. S. Tokat, I. Eksin, and M. Guzelkaya, ''New approaches for on-line tuning of the linear sliding surface slope in sliding mode controllers,'' Turkish J. Elect. Eng., vol. 11, no. 1, pp. 45–59, 2003.
17. F. Yorgancıoglu and H. Kömürcügil, ''Single-input fuzzy-like moving ˇ sliding surface approach to the sliding mode control,'' Electr. Eng., vol. 90, no. 3, pp. 199–207, Feb. 2008.
18. H. Komurcugil, ''Rotating-sliding-line-based sliding-mode control for single-phase UPS inverters,'' IEEE Trans. Ind. Electron., vol. 59, no. 10, pp. 3719–3726, Oct. 2012.
19. Brahmi, Brahim, Mohamed Hamza Laraki, Abdelkrim Brahmi, Maarouf Saad, and Mohammad H. Rahman. "Improvement of sliding mode controller by using a new adaptive reaching law: Theory and experiment." ISA transactions 97 (2020): 261-268.
20. Gao W, Hung JC. Variable structure control of nonlinear systems: A new approach. IEEE Trans Ind Electron 1993;40(1):45–55.
21. Fallaha CJ, Saad M, Kanaan HY, Al-Haddad K. Sliding-mode robot control with exponential reaching law. IEEE Trans Ind Electron 2011;58(2):600–10.

22. S. M. Mozayan, M. Saad, H. Vahedi, H. Fortin-Blanchette, and M. Soltani, ''Sliding mode control of PMSG wind turbine based on enhanced exponential reaching law,'' IEEE Trans. Ind. Electron., vol. 63, no. 10, pp. 6148–6159, Oct. 2016.
23. Y. Liu, Z. Wang, L. Xiong, J. Wang, X. Jiang, G. Bai, R. Li, and S. Liu, ''DFIG wind turbine sliding mode control with exponential reaching law under variable wind speed,'' Int. J. Electr. Power Energy Syst., vol. 96, pp. 253–260, Mar. 2018.
24. B. Brahmi, M. H. Laraki, A. Brahmi, M. Saad, and M. H. Rahman, ''Improvement of sliding mode controller by using a new adaptive reaching law: Theory and experiment,'' ISA Trans., vol. 97, pp. 261–268, Feb. 2020.
25. D. K. B. and S. Thomas, ''Power rate exponential reaching law for enhanced performance of sliding mode control,'' Int. J. Control, Autom. Syst., vol. 15, no. 6, pp. 2636–2645, Dec. 2017.
26. G. Rohith, ''Fractional power rate reaching law for augmented sliding mode performance,'' J. Franklin Inst., vol. 358, no. 1, pp. 856–876, Jan. 2021.
27. Zheng, Lijun, Fayang Jiang, Jiancheng Song, Yunguang Gao, and Muqin Tian. "A discrete-time repetitive sliding mode control for voltage source inverters." IEEE Journal of emerging and selected topics in power electronics 6, no. 3 (2017): 1553-1566.
28. Haroon, Faheem, Muhammad Aamir, and Asad Waqar. "Second-Order Rotating Sliding Mode Control with Composite Reaching Law for two level Single Phase Voltage Source Inverters." IEEE Access (2022).
29. Mian Qaisar, Saeed, "Baseline wander and power-line interference elimination of ECG signals using efficient signal-piloted filtering," Healthcare technology letters, vol. 7, no. 4, pp. 114–118, 2020.
30. S. M. Qaisar, S. I. Khan, D. Dallet, R. Tadeusiewicz, and P. Pławiak, "Signal-piloted processing metaheuristic optimization and wavelet decomposi-tion based elucidation of arrhythmia for mobile healthcare," Biocybernet-ics and Biomedical Engineering, vol. 42, no. 2, pp. 681–694, 2022.
31. S. M. Qaisar, "Efficient mobile systems based on adaptive rate signal pro-cessing," Computers & Electrical Engineering, vol. 79, p. 106462, 2019.
32. S. Mian Qaisar and F. Alsharif, "Signal piloted processing of the smart meter data for effective appliances recognition," Journal of Electrical En-gineering & Technology, vol. 15, no. 5, pp. 2279–2285, 2020.